THE JOURNAL OF PHYSICAL CHEMISTRY B

Article

pubs.acs.org/JPCB

Amino Acid Specific Effects on RNA Tertiary Interactions: Single-Molecule Kinetic and Thermodynamic Studies

Abhigyan Sengupta, Hsuan-Lei Sung, and David J. Nesbitt*

JILA, National Institute of Standards and Technology and Department of Chemistry and Biochemistry, University of Colorado, Boulder, Colorado 80309, United States

Supporting Information

ABSTRACT: In light of the current models for an early RNA-based universe, the potential influence of simple amino acids on tertiary folding of ribozymal RNA into biochemically competent structures is speculated to be of significant evolutionary importance. In the present work, the folding−unfolding kinetics of a ubiquitous tertiary interaction motif, the GAAA tetraloop−tetraloop receptor (TL−TLR), is investigated by single-molecule fluorescence resonance energy transfer spectroscopy in the presence of natural amino acids both *with* (e.g., lysine, arginine) and *without* (e.g., glycine) protonated side chain residues. By way of control, we also investigate the effects of a special amino acid (e.g., proline) and amino acid mimetic (e.g., betaine) that contain secondary or quaternary amine groups rather than a primary amine group. This combination permits systematic study of amino acid induced (or amino acid like) RNA folding dynamics as a function of side chain complexity, pK_a, charge state, and amine group content. Most importantly, each of the naturally occurring amino acids is found to *destabilize* the TL−TLR tertiary folding equilibrium, the kinetic origin of which is dominated by a *decrease* in the folding rate constant (k_{dock}), also affected by a strongly amino acid selective *increase* in the unfolding rate constant (k_{undock}). To further elucidate the underlying thermodynamics, single-molecule equilibrium constants (K_{eq}) for TL−TLR folding have been probed as a function of temperature, which reveal an amino acid dependent decrease in both overall exothermicity ($\Delta\Delta H^\circ > 0$) and entropic cost ($-T\Delta\Delta S^\circ < 0$) for the overall folding process. Temperature-dependent studies on the folding/unfolding kinetic rate constants reveal analogous amino acid specific changes in both enthalpy ($\Delta\Delta H^\ddagger$) and entropy ($\Delta\Delta S^\ddagger$) for accessing the transition state barrier. The maximum destabilization of the TL−TLR tertiary interaction is observed for arginine, which is consistent with early studies of arginine and guanidine ion-inhibited self-splicing kinetics for the full *Tetrahymena* ribozyme [Yarus, M.; Christian, E. L. *Nature* **1989**, *342*, 349−350; Yarus, M. *Science* **1988**, *240*, 1751−1758].

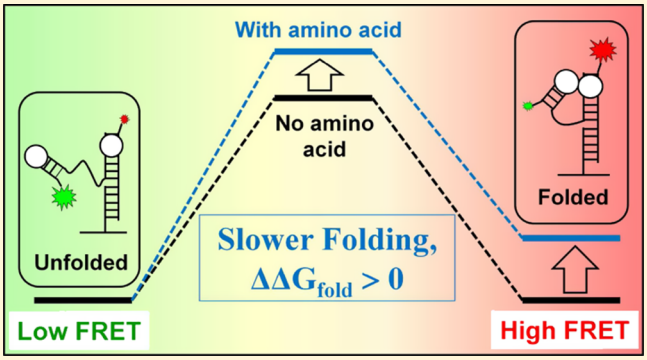

I. INTRODUCTION

Noncoding RNA has been found to play a key role in an ever-widening array of biochemical processes critical in cellular biology, including gene expression, gene modification, and gene repair.[1,2] A crucial part of the functional diversity of such noncoding RNA lies in its ability to fold into compact and biochemically competent structures, such as small interfering RNA;[3,4] larger structure-forming domains, such as ribos-witches;[5−7] and even much larger ribonucleoprotein complexes, such as the ribosome.[8−10] In each of these processes, the strength and specificity of interaction between RNA and proteins represent essential properties of biological relevance.[2] What makes this particularly interesting is that this could not have always been the case, specifically in the early evolutionary stages of life on earth.[11−16] Indeed, in the RNA-dominated world some 4 billion years ago, neither complex proteins nor simple amino acid building blocks of proteins were thought to be present.[14] Instead, the simplest catalytic processes were carried out by RNA-based enzymes (i.e., ribozymes), as first demonstrated in the pioneering work by Cech and co-workers[17] on self-splicing RNA in the *Tetrahymena* group I intron. Recent studies on self-replicating RNA strands inside vesicles also support this "RNA first" concept.[16,18−21]

By way of comparison, introduction of amino acids into the biosphere is thought to have occurred much later than that of RNA,[11,14,22] which eventually triggered evolution toward more efficient protein-based enzymes and the domination of cellular biology by the central dogma of genomic DNA → mRNA → proteins. What makes this particularly interesting is that there must have been considerable overlap of evolutionary epochs, where biochemically active RNA ribozymes were continually being exposed to simple amino acids and even small polypeptide sequences. It is therefore not implausible and

Received: June 9, 2016
Revised: August 30, 2016
Published: October 10, 2016

DOI: 10.1021/acs.jpcb.6b05840
J. Phys. Chem. B 2016, 120, 10615−10627

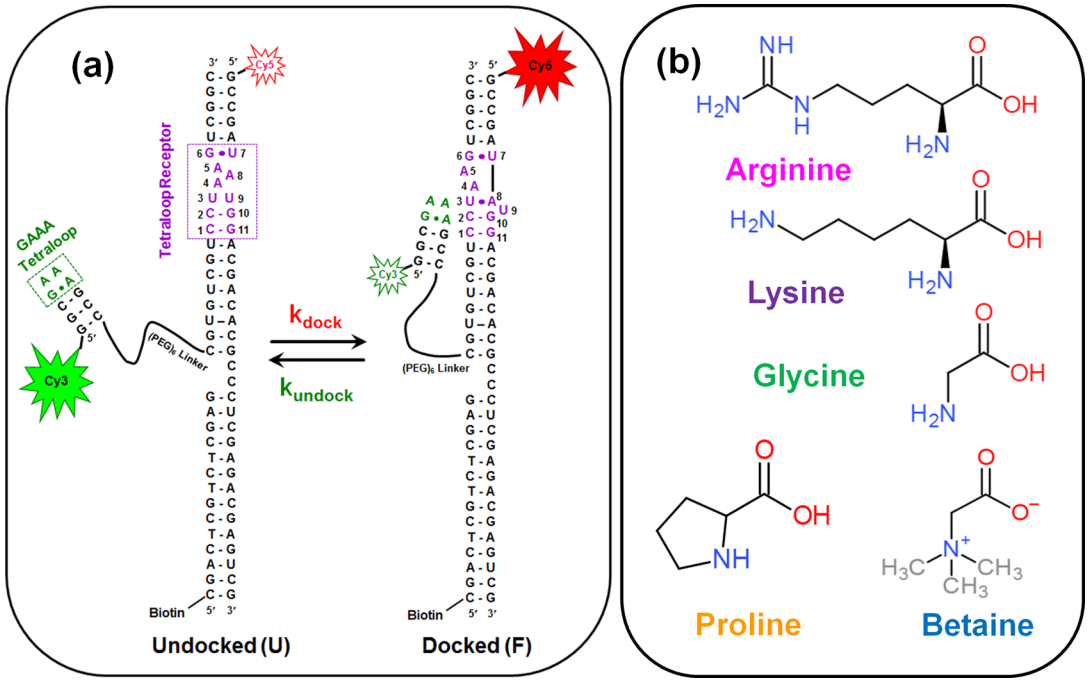

Figure 1. (a) Schematic representation of the TL−TLR interaction, for which changes in the FRET efficiency (E_{FRET}) between Cy3 and Cy5 allow one to probe the folding−unfolding dynamics of the RNA construct. (b) Chemical structures of the three naturally occurring amino acids (Arg, Lys, Gly), a secondary-amine-containing special amino acid (Pro), and an amino acid mimetic (Bet) used in the present study.

even quite likely that evolutionary pressure to develop the first pathways for protein synthesis and the eventual predominance of protein-based enzymatic activity would be based on the influence of amino acids on RNA function. If this is indeed the case, then the fundamental amino acid−RNA interactions and, in particular, the way this interaction could be responsible for steering biology from an RNA- to protein-dominated biological machinery, would be of major evolutionary relevance.

The potential relevance of such RNA−protein binding interactions has long been appreciated. In the early 1960s, research with genetic coding by Woese[23] and Orgel[24] triggered interest in the critical nature of the RNA−amino acid interaction. Specifically, the crucial importance of RNA−amino acid interactions was explored in the context of ribosomal protein synthesis.[25] More recently, researchers have detected riboswitches with high specific affinities for amino acids, which can trigger the folding of the overall riboswitch to either promote or inhibit gene transcription. The methionine riboswitch,[26−28] lysine riboswitch,[29,30] citruline aptamer,[31] and arginine riboswitch[31,32] are but a few examples of such amino acid specific binding RNAs. Indeed, the presence of amino acid metabolite-based riboswitches could be considered additional evidence for the evolutionary importance of RNA−amino acid interactions.

Although several amino acid binding RNA sequences have been identified,[26−32] the role of amino acids in influencing the folding kinetics is not well understood. An early experimental clue to amino acid control of RNA enzymatic activity was reported by Yarus and Christian[33,34] in 1988, wherein they detected a reversible amino acid binding site in the *Tetrahymena* group I intron.[33−35] Specifically, increasing concentrations of L-arginine were reported to *inhibit* the self-splicing catalytic activity of the *Tetrahymena* ribozyme.[33−35] Such arginine-inhibited RNA splicing dynamics provided intriguing first support for the potential importance of RNA−amino acid interactions in the steering of actual biological processes.

To date, researchers have obtained invaluable information about the geometry and orientation of several RNA−amino acid complexes using high-resolution three-dimensional imaging techniques[36−39] and quantum mechanical ab initio calculations.[40−42] However, these results crucially do not provide kinetic and thermodynamic data relevant to RNA folding and unfolding. Specifically, RNA is highly dynamic, and consequently, its biological function depends on time-dependent conformational changes.[43,44] Therefore, to elucidate the potential effects on RNA biofunctionality, it is of special importance to systematically explore the *single-molecule kinetics* of RNA folding−unfolding in the presence of amino acids. Moreover, amino acids could influence either secondary or tertiary RNA structure formation, which is especially relevant, as RNA folding is hierarchical, distinguished by fast secondary-structure formation (μs to ms), followed by tertiary folding on a much slower time scale (ms to s to min).[45−48] It is therefore important to probe for amino acid contributions to both structural contributions in isolation, the first step of which we achieve in this work by focusing a single, ubiquitous RNA tertiary motif. It is worth stressing that the *kinetics* of RNA structural changes is of particular interest, as amino acids could, in principle, impact either the *folding* or *unfolding* kinetic pathway, only the ratio of which is detected under bulk equilibrium conditions.[33,35] Finally, complete temperature-dependent kinetic and thermodynamic information would clearly be useful, permitting separate enthalpic (ΔH) and entropic ($-T\Delta S$) contributions to the free-energy (ΔG) landscape for RNA tertiary folding/unfolding to be determined as a function of amino acid concentration and identity. Indeed, it is the detailed implementation and analysis of such a combined temperature-dependent kinetic and thermodynamic

DOI: 10.1021/acs.jpcb.6b05840
J. Phys. Chem. B 2016, 120, 10615−10627

study at the single-molecule level that represent the major focus of this article.

In the current work, we explore the GAAA tetraloop−tetraloop receptor (TL−TLR), a ubiquitous tertiary motif and key structural element in the P4−P6 domain of the *Tetrahymena* ribozyme, as a model system for the effects of amino acids on RNA tertiary interactions. Specifically, we have studied the kinetic and thermodynamic influences on RNA folding of three natural amino acids (glycine, lysine, and arginine), one special amino acid (proline), and one amino acid mimetic (betaine) of increasing complexity, pK_a, charge state, and amino content (primary to secondary to quaternary), using single-molecule fluorescence resonance energy transfer (smFRET) and time-correlated single-photon counting (TCSPC) methods.[49] The folding/unfolding rate constants and equilibrium constants for the TL−TLR interaction are explored as functions of temperature and concentration. Each of the naturally occurring amino acids is found to strongly *destabilize* the overall tertiary folding process, specifically by *decreasing* the rate constant (k_{dock}) for folding, with only relatively minor effects on the unfolding rate constant (k_{undock}) due to glycine and lysine. Interestingly, arginine behaves quite differently from the other two natural amino acids by also strongly *increasing* the unimolecular unfolding rate (k_{undock}). It is especially worth noting that such arginine-selective inhibition of TL−TLR folding would be in good agreement with previous reports[33−35] on inhibition of self-splicing kinetics for the full *Tetrahymena* ribozyme.

Furthermore, temperature-dependent experiments permit us to analyze the free energies for such amino acid inhibited TL−TLR folding/unfolding kinetics as *enthalpic* and *entropic* contributions. In general, all three primary-amine-containing natural amino acids (glycine, lysine, and arginine) are found to (1) *decrease* the enthalpic advantage and (2) *lower* the entropic cost of folding, whereas the special amino acid (proline) and the amino acid mimetic (betaine) reveal significantly smaller or a negligible impact on the equilibrium/kinetic properties. Although restricted in the number of species explored, this work provides first insights into how amino acids with varying side chain complexities, pK_a's, charge states, and amino group contents influence the folding/unfolding kinetics and equilibrium properties of a fundamental RNA tertiary interaction. Of potentially the greatest interest, we find that even the simplest amino acid (glycine) is able to significantly impact the RNA folding kinetics, which would be relevant to the importance of amino acid based evolution in an early RNA-dominated world.

II. MATERIALS AND METHODS

II.A. Fluorescent TL−TLR RNA Design and Sample Preparation. TL−TLR (see Figure 1a) is used as a model RNA to investigate the effects of a few selected amino acids (Figure 1b) on this ubiquitous loop−bulge tertiary interaction. Arginine is the obvious first choice of amino acid by virtue of the studies by Yarus.[33] Lysine represents the natural control for comparison of effects due to the presence of the guanidinium moiety versus a solely cationic side chain. As the simplest amino acid, glycine constitutes a logical control for any contribution due to zwitterionic effects. The studies with proline and betaine reflect additional controls for the amino acid moiety, on the basis of modifying the amino group from primary to secondary to quaternary. All of these choices were further influenced by solubility considerations. Details of the RNA design and biophysical characterization have been reported previously.[50−54] To eliminate the effects due to possible base stacking in the linker, the TL−TLR constructs used in the present studies have been slightly modified by replacing the central RNA linker (U7 or A7) with a flexible hexamer polyethylene glycol (PEG_6) linker to join the tetraloop and receptor domain (Figure 1a). The RNA construct is then assembled by annealing three commercially purchased oligonucleotides (Integrated DNA Technologies): (1) a Cyanine 3 (Cy3)-labeled RNA strand (5′-Cy3-GGCGA-AAGCC-PEG_6-CGUGUCGUCCUAAGUCGGC-3′), (2) a Cynanine 5 (Cy5)-labeled RNA strand (5′-GCCGAUAUGGA-CGACACGCCCUCGAGACGAGUCG-3′), and (3) a 14-nucleotide, 5′-biotinylated DNA strand (5′-biotin-CGCACTCGTCTGAG-3′). The method of purification has been described previously in the literature.[55]

For the smFRET experiments, the RNA constructs are attached to a glass coverslip through biotin−streptavidin interactions (see Figure 2 inset). The RNA attachment is

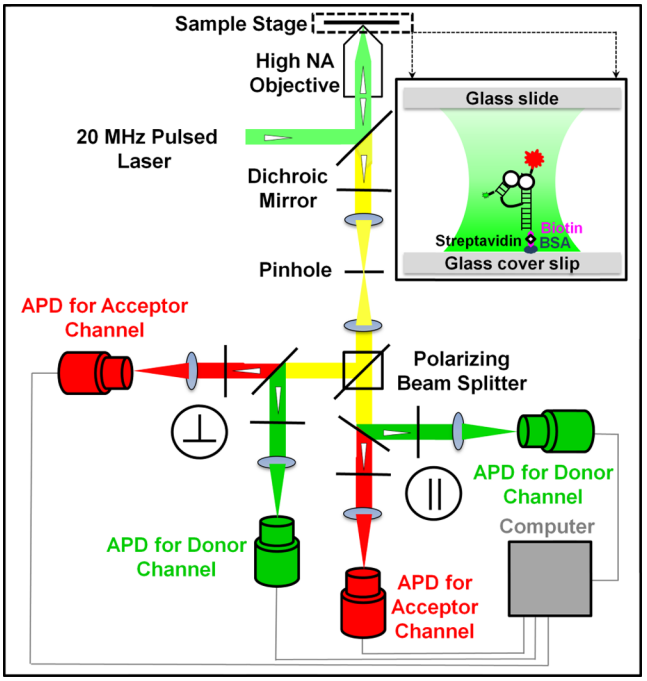

Figure 2. Schematic of the single-molecule confocal fluorescence microscope. Inset: Biotin−streptavidin method for surface-tethering of individual RNA molecules in solution on a glass coverslip.

achieved by sequential flushing with three solutions: (1) 10 mg/mL bovine serum albumin (BSA), containing 10% biotinylated BSA; (2) 200 μg/mL streptavidin solution; and (3) 50 pM biotinylated TL−TLR construct. A 10 min incubation time is allowed after each step, a procedure that achieves a uniform average surface coverage of ≈1 molecule/μm^2. Prior to imaging under a fluorescence microscope, the sample channel is flushed with 200 μL of scavenger solution, containing (1) 50 mM hemisodium *N*-(2-hydroxyethyl)-piperazine-*N*′-propanesulfonic acid (HEPES) buffer, (2) 2 mM 9-hydroxy-2,5,7,8-tetramethylchroman-2-carboxylic acid (TROLOX), (3) 100 nM protocatechuate 3,4-dioxygenase, and (4) 5 mM protocatechuic acid (3,4-dihydroxybenzoic acid). This solution serves as a catalytic oxygen scavenger and thereby extends the single-molecule fluorescence trajectory lifetimes by minimizing photobleaching effects.[56] Experiments are per-

DOI: 10.1021/acs.jpcb.6b05840
J. Phys. Chem. B 2016, 120, 10615−10627

formed in 50 mM HEPES buffer (pH 7.5), with a 85 mM total concentration of monovalent ions (Na^+ and K^+). The present study is constrained to a single set of cationic conditions (specifically, a constant monovalent concentration), with changes only in the amino acid (1) species and (2) concentration. The buffer contains no Mg^{2+}, which opens a larger dynamic range of amino acid concentrations for exploration. For each experiment, the desired concentration (0−1000 mM) of a specific amino acid or amino acid mimetic in buffer is combined with small volumes of the scavenger cocktail and flushed through the sample chamber.

II.B. Single-Molecule Fluorescence Confocal Microscope. A schematic diagram of a single-molecule fluorescence confocal microscope (Olympus IX-70)[53] is shown in Figure 2. Samples are illuminated by a mode-locked, frequency-doubled Nd:YAG pulsed laser, which operates at a 20 MHz repetition rate and emits 532 nm (green) pulses. The green laser beam is then expanded to overfill the back aperture of the objective and focused onto a diffraction-limited spot in the sample chamber through a 1.2 NA water-immersion objective (UPlanApo 60×; Olympus, Center Valley, PA). Average laser power can be varied from 0.05 to 100 μW by neutral-density filters, with sample excitation and fluorescence photon collection performed through the same objective. A dichroic mirror reflects scattered excitation light away from the sample detectors, focusing the emission through a 50 μM spatial filter pinhole and reimaging through (1) a polarization beam cube (CVI PBSH-450-1300-100; CVI Laser Optics, Albuquerque, NM) and (2) two matched dichroic filters (645DCXR; Chroma Technology, Bellows Falls, VT) onto four single-photon-counting avalanche photodiodes (APDs; SPCM-AQR-14; Perkin-Elmer Optoelectronics, Fremont, CA). Which detector the photon strikes is therefore determined by both the (1) polarization (horizontal vs vertical) and (2) wavelength (donor or acceptor) of the single-photon emission event. The APD signals are recorded with a TCSPC module (SPC-134; Becker & Hickl, Berlin, Germany), which measures the arrival time of each photon relative to the excitation laser pulse (τ_{micro}, $\Delta\tau$ < 200 ps) as well as the start of the data collection period (τ_{macro}, $\Delta\tau$ = 50 ns). All 4 bits of photon information (horizontal vs vertical, donor vs acceptor, τ_{macro}, τ_{micro}) are stored in memory and analyzed with in-house software, which permits complete flexibility in recreating two-dimensional scanning images and/or fluorescence trajectories in time. For the temperature-dependent studies, the Teflon chamber is mounted on a stage heater (HCS60; INSTEC, Boulder, CO), with a resistive collar (Bioptechs, Butler, PA) to heat the microscopic objective.[54,57−59] The temperatures of both the objective and heater are maintained by proportional, integral, and derivative servo loop control and measured to be stable up to ±0.1 °C.

III. RESULTS AND ANALYSIS

III.A. Amino Acids Destabilize the Folded State by *Slowing* the Folding Rate Constants. Sample fluorescence trajectories for an isolated TL−TLR construct in the absence and presence of 100 mM arginine are presented in Figure 3a, which clearly shows a two-level fluorescence intensity as the RNA interconverts between the folded and unfolded states. The FRET efficiency (E_{FRET}) is determined from the fractional intensity of the acceptor fluorescence, with Figure 3b displaying a sample time-dependent E_{FRET} trajectory. The low (E_{FRET} ≈ 0.30) and high (E_{FRET} ≈ 0.75) FRET states correspond to unfolded and folded TL−TLR conformers, respectively. Note

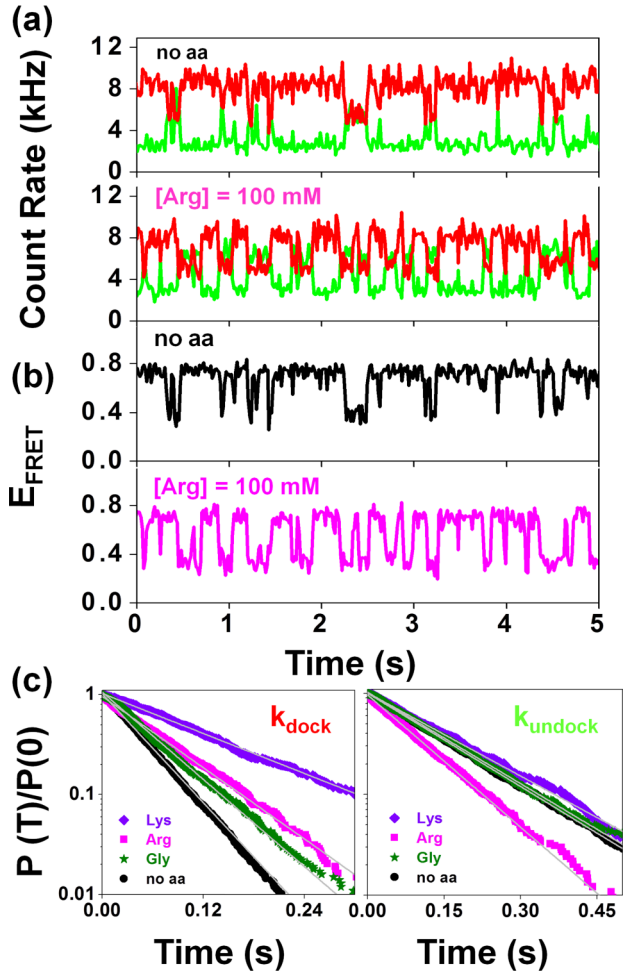

Figure 3. (a, b) Fluorescence intensity trajectories (in kHz) and corresponding E_{FRET} trajectories illustrate two distinct conformers of RNA, both in the presence (100 mM) and absence (0 mM, "no aa") of arginine. (c) Cumulative distribution functions obtained from a dwell time analysis, which, based on the four-state kinetic model, is well characterized by purely single exponential decay. Folding (k_{dock}) and unfolding (k_{undock}) rate constants (no aa and 100 mM) are obtained by analyzing multiple E_{FRET} trajectories from a sufficiently large (>30) ensemble of RNA molecules.

that in the absence of the amino acid, the folded state (E_{FRET} ≈ 0.75) is predominantly observed, with the fluorescence traces revealing only short transient excursions into the unfolded (E_{FRET} ≈ 0.30) state. By way of contrast, in the presence of 100 mM arginine, the frequency of such excursions to the low-FRET state increases significantly (Figure 3b), with similar changes noted for 100 mM lysine and 100 mM glycine (Figure S1). This immediately implies that the presence of each of these three natural amino acids *destabilizes* the folded state of the TL−TLR tertiary construct.

The distribution of dwell times spent in the high- versus low-FRET states contains detailed rate constant information on the RNA folding and unfolding kinetics. To achieve a high statistical accuracy, we exploit the cumulative probability distributions[60] of these dwell times from a sample size of 30−50 individual molecules (Figure 3c). As expected for a simple first-order kinetic process, the normalized probability densities ($P(\tau)/P(0)$) are well described by a single exponential decay, with slopes yielding folding (k_{dock}) and unfolding (k_{undock}) rate constants.[61,62] The influence of amino acid

DOI: 10.1021/acs.jpcb.6b05840
J. Phys. Chem. B 2016, 120, 10615−10627

concentration on TL−TLR folding is clearly evident, notably dominated by a significant *decrease* in k_{dock}. Specifically, the folding rate constant in the absence of amino acid (k_{dock} = 21.5(13) s^{-1}) decreases by ≈2.5 fold (k_{dock} = 8.6(9) s^{-1}) due to 100 mM lysine, with similar, albeit slightly weaker, decreases observed for arginine (k_{dock} = 13.6(3) s^{-1}) and glycine (k_{dock} = 15.2(6) s^{-1}). Interestingly, however, the corresponding amino acid concentration effects on unimolecular *unfolding* are essentially negligible for both lysine and glycine, with arginine accounting for a moderate but clear *increase* in the unfolding rate constant (k_{undock} = 9.7(6) s^{-1} vs 6.7(2) s^{-1}). Indeed, it is also worth noting that the synergism between (1) slower folding and (2) more rapid unfolding makes the influence of arginine the strongest among that of the amino acids studied. This provides a useful confirmation of trends noted previously by Yarus and co-workers, who reported that the presence of arginine significantly destabilizes the catalytic self-splicing activity of the Tetrahymena ribozyme.[35] In all cases, however, the equilibrium shift behavior is dominated by a *decrease* in the docking rate constants rather than *increase* of the undocking rate constants, which makes clear predictions for shifts in overall free-energy changes and transition state free-energy barriers.

III.B. Four-State Kinetic Analysis of TL−TLR Folding/Unfolding Rates. To establish an underlying kinetic model for such behavior, we consider the dependence of folding and unfolding rate constants on amino acid concentration, as summarized in Figure 4. All folding rate constants, k_{dock}, *decrease* with increasing amino acid concentration and saturate at a high concentration. In contrast, k_{undock} values remain nearly flat for [lysine] and [glycine], whereas [arginine] exhibits a modest increase in the unfolding rate constant and eventually saturates. Neither folding nor unfolding behavior is consistent with the simple elementary rate process, which would always predict a linear dependence of the first-order rate constants on concentration. Instead, such kinetic behavior signals arise from concentration-dependent competition between (1) amino acid−RNA binding and (2) TL−TLR folding events. Therefore, to extract the kinetic information, a widely used four-state model (Figure 5) for metabolite-dependent RNA folding and unfolding is employed.[58,63,64] This kinetic model assumes (1) *rapid* amino acid equilibration with both the folded (A + F ↔ FA) and unfolded (U + A ↔ UA) conformers, (2) indistinguishable FRET values for amino acid bound/unbound states (e.g., U, UA), and (3) *slower* tertiary folding/unfolding of the TL−TLR RNA. In the context of such a model, the cumulative probability distributions are again single-exponential, with effective docking/undocking rate constants given by an equilibrium-weighted average over the each of the amino acid unassociated ($k_{1/-1}$) and associated ($k_{2/-2}$) pathways. Specifically

$$k_{dock/undock} = \frac{k_{1/-1}}{1 + K_{f/u}[A]} + \frac{k_{2/-2}K_{f/u}[A]}{1 + K_{f/u}[A]} \quad (1)$$

where the association constants for the folded and unfolded TL−TLR RNA conformers are given by $K_f = \frac{[UA]}{[U][A]}$ and $K_u = \frac{[FA]}{[F][A]}$, respectively (see Figure 5c). Note that eq 1 predicts the physically correct asymptotic limiting behavior for both $K_{f/u}[A] \gg 1$ and $K_{f/u}[A] \ll 1$.

Least squares analysis of the amino acid dependent rate constant data to eq 1 permits folding (k_{dock}) and unfolding (k_{undock}) rate constants as well as association constants ($K_{f/u}$) to be determined, with the fit predictions plotted in Figure 4. For lysine and glycine, the kinetic model accurately captures the rate constant trends over the full concentration range, with the observed folding rate constant decreasing smoothly to an asymptotic value under saturating conditions. The folding rate constant for arginine decreases smoothly from 0 to 300 mM to a saturation value and slowly rises by 10−15% up to 600 mM, which likely reflect additional cooperative interactions between more than one arginine and TL−TLR favored at higher concentrations. Thus, to be consistent with the simple four-state model, the arginine data are least squares fit over the 0−300 mM range, with the results for all amino acid (and amino acid mimetic) species quantitatively summarized in Table 1. As expected, the rate constants for the *unassociated* TL−TLR construct (k_1 and k_{-1}) reveal no sensitivity to amino acid identity. Table 1 also shows a very clear concentration-dependent *decrease* in the folding rate constant (i.e., $k_2 < k_1$) in the presence of each amino acid, with a much smaller dependence of the undocking rate constant on concentration for lysine and glycine (i.e., $k_{-1} \approx k_{-2}$). Interestingly, only arginine shows a significant concentration-dependent *increase* in the unfolding rate constant (i.e., $k_{-1} < k_{-2}$).

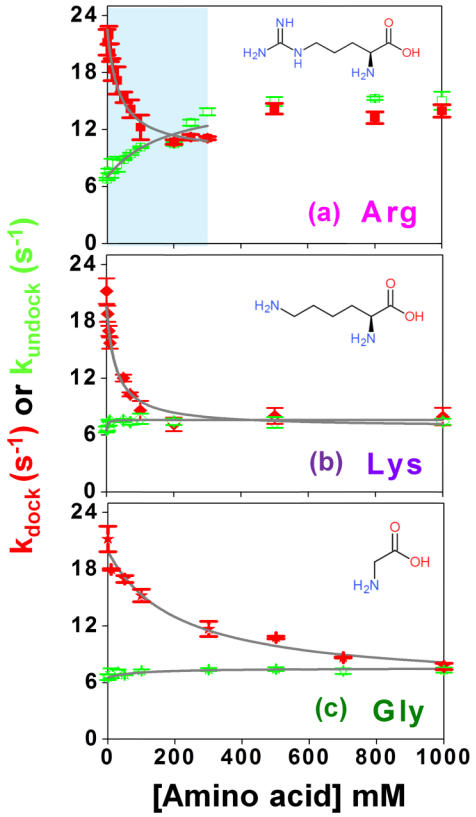

Figure 4. Folding (k_{dock}) and unfolding (k_{undock}) rate constants for TL−TLR RNA, plotted as a function of [amino acid]. The solid lines represent least squares fits to the four-state kinetic model (see Figure 5 and text for details). A slight increase in the folding rate constant (k_{dock}) for arginine is observed at higher concentrations. For consistency with the kinetic model, we restrict fits to the arginine data to 300 mM.

Figure 6 summarizes the results for the resulting dependences of the overall effective folding equilibrium constant (K_{eq} = k_{dock}/k_{undock}) on amino acid concentration. As expected from the above discussion, the steep decrease in the docking rate

DOI: 10.1021/acs.jpcb.6b05840
J. Phys. Chem. B 2016, 120, 10615−10627

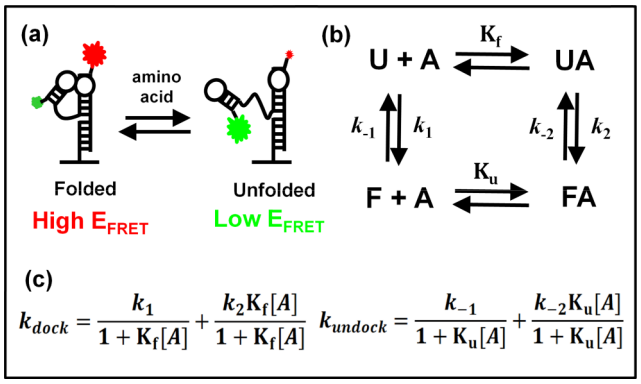

Figure 5. (a) Cartoon representation of the folded and unfolded conformers of TL−TLR RNA, where the RNA tertiary structure is unfolded by amino acids. (b) The four-state kinetic model describes the origin of the amino acid dependent folding−unfolding behavior of the RNA tertiary structure. U, F, A, UA, and FA represent the unfolded, folded, amino acid, amino acid bound unfolded, and amino acid bound folded states, respectively. k_1/k_2 and k_{-1}/k_{-2} reflect the forward and reverse rate constants for the unassociated/associated species, respectively, with $K_{f/u}$ representing the equilibrium association constants. Experiments measure only the *effective rate constant* for net unfolding/folding (k_{undock} and k_{dock}), which is not the same as $k_{1/-1}$, $k_{2/-2}$ but in our kinetic model can be expressed as a function of these plus the association/dissociation equilibrium constants. (c) Expressions for the effective folding (k_{dock}) and unfolding (k_{undock}) rate constants derived from the four-state kinetic model and used to fit the amino acid dependent changes.

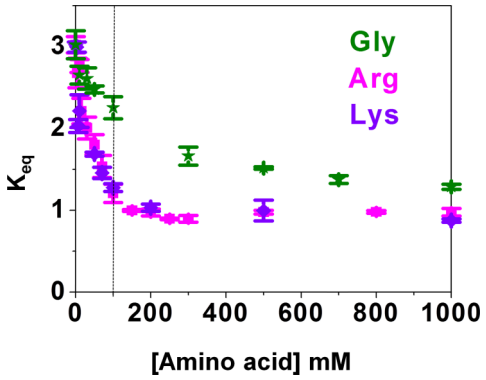

Figure 6. Folding equilibrium constant (K_{eq}) for TL−TLR RNA plotted as a function of amino acid concentration. K_{eq} is obtained from the ratio of collective dwell times spent by RNA in the folded vs unfolded states.

constant for each of the amino acids results in a similarly steep decrease in K_{eq}, although the K_f values for arginine and lysine are 10-fold smaller than those of glycine and therefore the impact on the folding kinetics is considerably more pronounced at low concentrations. The rapid decrease in these equilibrium constants confirms that the presence of amino acids *destabilizes* tertiary folding in the TL−TLR construct, driven mostly by a slowing of the folding rate constant. These equilibrium constants can be quantified with the simple expression $\Delta G^\circ = -RT\ln(K_{eq})$ to infer standard-state free-energy changes (Table 2) for the tertiary folding process. In the absence of amino acids, the free-energy change associated with folding ($\Delta G^\circ_{fold,0} < 0$) is a spontaneously allowed process.[59] However, concentrations at the 100−200 mM level enhance this free-energy change to nearly thermoneutral or even slightly uphill ($\Delta\Delta G^\circ > 0$; see Table 2), consistent with amino acid induced *destabilization* of the TL−TLR tertiary interaction.

III.C. Temperature-Dependent Amino Acid Induced TL−TLR RNA Folding. It is particularly instructive to explore the thermodynamic origins for such an amino acid destabilized folding of the TL−TLR tertiary interaction, which can be obtained from *temperature-dependent* measurements at the single-molecule level. Specifically, the standard-state free-energy change (ΔG°_{fold}) can be resolved into enthalpic (ΔH°) and entropic ($-T\Delta S^\circ$) contributions by the van't Hoff equation[54]

$$\ln K_{eq} = -\frac{\Delta G^\circ_{fold}}{RT} = \frac{\Delta S^\circ}{R} - \frac{\Delta H^\circ}{RT} \quad (2)$$

where R is the ideal gas constant and T represents temperature in the Kelvin scale. A plot of $\ln K_{eq}$ versus $1/T$ yields a straight line for each set of experiments, with the slope and intercept being $-\frac{H^\circ}{R}$ and $\frac{S^\circ}{R}$, respectively.

The corresponding van't Hoff plots for the TL−TLR construct with and without 100 mM amino acid are shown in Figure 7, yielding the least squares fitted thermodynamic parameters summarized in Table 2. Inspection of the slopes immediately indicates that TL−TLR folding is a substantially exothermic process ($\Delta H^\circ < 0$), consistent with previous studies.[59] Note that the presence of each amino acid induces only a relatively small shift in this slope, in a direction that reduces the overall folding exothermicity ($\Delta\Delta H^\circ > 0$). However, the more dominant thermodynamic effect would appear to be the strong downward and nearly equivalent shifts in the van't Hoff intercepts (i.e., $-T\Delta\Delta S^\circ < 0$) observed for lysine and arginine. For these high-pK_a long-chain residue species, the source of such an amino acid dependent destabilization is clearly *entropic* in nature. Interestingly, there is a much smaller shift in the van't Hoff intercept for the much simpler amino acid glycine, which would be consistent with ascribing the predominant destabilization effects to the higher pK_a values of the arginine and lysine residues.

To explore the corresponding kinetic effects of amino acids on the TL−TLR transition state dynamics, we have investigated folding/unfolding rate constants as a function of temperature.

Table 1. Docking (k_1/k_2), Undocking (k_{-1}, k_{-2}), Rate Constants and Equilibrium Constants (K_a, K_b) Derived from the Four-State Kinetic Model (Shown in Figure 5) for Amino Acid Concentration-Dependent Folding of TL−TLR RNA

	k_1 (s^{-1})	k_2 (s^{-1})	k_{-1} (s^{-1})	k_{-2} (s^{-1})	K_f (mM^{-1})	K_u (mM^{-1})
arginine	22(2)	9.4(5)	6.9(3)	16(2)	0.032(12)	0.006(3)
lysine	20(1)	6(1)	6.8(2)	7.4(3)	0.035(12)	0.7(2)
glycine	20(1)	5.5(15)	6.6(2)	7.3(3)	0.004(1)	0.04(3)
betaine	21(1)	6.7(5)	6.8(1)	8.6(5)	0.67(5)	0.6(2)
proline	20(1)	22(1)	6.6(1)	7(1)	0.016(4)	0.02(1)

[a]Uncertainties (1σ) in the final decimal place are listed in parentheses.

DOI: 10.1021/acs.jpcb.6b05840
J. Phys. Chem. B 2016, 120, 10615−10627

Table 2. Thermodynamic Parameters Obtained from van't Hoff Analysis and Transition-State Analysis for Different Amino Acids (at 100 mM) from the Temperature-Dependent Experiments

	ΔG°_{fold} (kcal/mol) at 298 K	ΔH°_{fold} (kcal/mol)	ΔS°_{fold} (cal/mol K)	$\Delta\Delta G^{\ddagger}_{fold}$ (kcal/mol) at 298 K	$\Delta H^{\ddagger}_{fold}$ (kcal/mol)	$\Delta\Delta S^{\ddagger}_{fold}$ (cal/mol K)
no aa	−0.65(3)	−33(1)	−110(4)	[a]	−7(1)	[a]
arginine	−0.11(5)	−25(2)	−86(5)	0.32(7)	−6(1)	4(2)
lysine	−0.14(2)	−28(1)	−95(2)	0.53(8)	−1(1)	19(5)
glycine	−0.48(4)	−29(2)	−98(6)	0.20(5)	−10(1)	−11(5)
betaine	−0.35(3)	−32(2)	−107(6)	0.20(4)	−3(1)	14(4)
proline	−0.57(3)	−26(4)	−87(13)	0.01(4)	−16(2)	−31(7)

[a]Due to lack of precision information on the attempt frequency, ν, only $\Delta\Delta G^{\ddagger}_{fold}$ and $\Delta\Delta S^{\ddagger}_{fold}$ values are determined rigorously and therefore reported. However, for an assumed value of $\nu \approx 10^{-13}$ s^{-1}, $\Delta G^{\ddagger}_{fold} \approx 15.92(4)$ kcal/mol and $\Delta S^{\ddagger}_{fold} \approx -77(2)$ cal/mol K in the absence of amino acid.

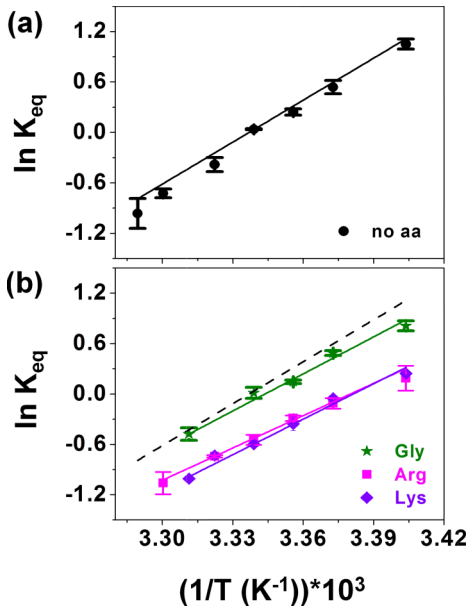

Figure 7. van't Hoff plot of the temperature-dependent TL−TLR folding equilibrium constant (a) without and (b) with 100 mM amino acid. The lines are obtained by fitting each data set to a linear function to extract ΔH° and ΔS° from the slopes and intercepts, respectively.

According to generalized transition state theory, the rate constant can be written in the Arrhenius form as

$$k = \nu \exp \frac{-\Delta G^{\ddagger}}{RT} \tag{3}$$

where $\Delta G^{\ddagger}$ is the transition state free energy and ν reflects the "attempt frequency" along the reaction coordinate to access the transition state barrier.[65,66] The above expression can be resolved into enthalpic ($\Delta H^{\ddagger}$) and entropic ($\Delta S^{\ddagger}$) contributions

$$\ln k = \ln \nu + \frac{\Delta S^{\ddagger}}{R} - \frac{\Delta H^{\ddagger}}{RT} \tag{4}$$

where $\Delta H^{\ddagger}$ and $\Delta S^{\ddagger}$ now represent changes in enthalpy and entropy between the folded (or unfolded) species and transition state, respectively. $\Delta H^{\ddagger}$ can be obtained rigorously from the temperature-dependent slopes versus $1/T$. In the absence of detailed molecular dynamics calculations, ν is often very roughly assumed to be on the order of 10^{13} s^{-1}.[67,68] However, as the transition state entropy depends only *logarithmically* on the attempt frequency, this uncertainty in ν maps onto a very small range of $\Delta S^{\ddagger}$. More relevantly, any amino acid induced *differences* in the barrier free energy ($\Delta\Delta G^{\ddagger}$) and entropy ($\Delta\Delta S^{\ddagger}$) are rigorously insensitive to this estimate of ν, which are therefore the appropriate quantities reported in Table 2.

The resulting Arrhenius plots of $\ln k_{dock}$ versus $1/T$ are summarized in Figure 8, with the corresponding thermodynamic parameters listed in Table 2. The slope determines $-\frac{\Delta H^{\ddagger}}{RT}$ and the intercept contains information on $\Delta\Delta S^{\ddagger}$. Simple inspection of $\ln k_{dock}$ versus $1/T$ reveals that TL−TLR access to the transition state in the absence of amino acid is (1) weakly exothermic ($\Delta H^{\ddagger} < 0$) and (2) entropically costly ($\Delta S^{\ddagger} < 0$). In an emerging theme with the van't Hoff equilibrium constant analysis above, both arginine and lysine reduce the exothermicity ($\Delta\Delta H^{\ddagger} > 0$) as well as decrease the entropic barrier ($-T\Delta\Delta S^{\ddagger} < 0$) for accessing the TL−TLR transition state. Yet again, quite opposite effects are observed for glycine, for which TL−TLR access to the folding TS becomes more exothermic ($\Delta\Delta H^{\ddagger} < 0$) and increases the entropic barrier ($-T\Delta\Delta S^{\ddagger} > 0$). In summary, there is a consensus in the overall free-energy outcome for destabilization, although with clear selectivity in amino acid induced enthalpy and entropy changes for TL−TLR folding.

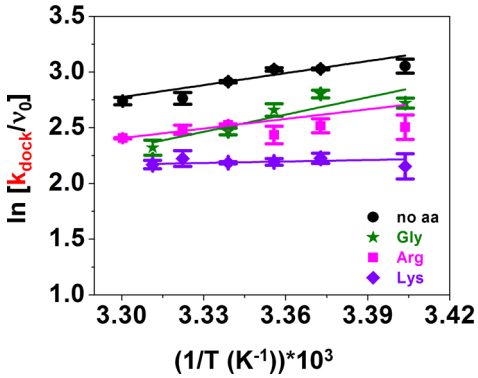

Figure 8. Transition state analysis of folding rate constant (k_{dock}) with and without amino acid. The individual lines are obtained by fitting each data set to a linear function to infer $\Delta H^{\ddagger}$ and $\Delta\Delta S^{\ddagger}$.

IV. DISCUSSION

IV.A. Influence of Amino Acids on TL−TLR Folding/Unfolding Kinetics. The functional competence of a ribozyme is strongly coupled to the folding−unfolding kinetics of the associated RNA, for which destabilization of the fully folded state will lead to inhibition of biochemical activity.[17,69−73] Previously, Yarus and co-workers reported that the presence of arginine inhibits the self-splicing activity of the *Tetrahymena* ribozyme.[33−35] In addition, they also observed

DOI: 10.1021/acs.jpcb.6b05840
J. Phys. Chem. B 2016, 120, 10615−10627

that the positively charged free guanidine ion by itself in solution inhibits self-splicing of the *Tetrahymena* ribozyme,[35] which would suggest a simple "moiety-specific" physical picture of the underlying biochemical inhibition pathway. Their work has served as stimulus for the present study, specifically toward probing the influence of structurally diverse amino acids (Figure 1b) on the same TL−TLR tertiary interaction[51,53,54,64,74] responsible for folding the catalytically active P4−P6 domain in the *Tetrahymena* ribozyme. Within the limits imposed by solubility, the experimental strategy has been to isolate the fundamental tertiary interaction involved and explore the amino acid induced impact of (1) moiety identity, (2) charge/pK_a, (3) residue chain length, and (4) amino and carboxylic acid functional groups on the inhibition of TL−TLR folding.

First, we focus on arginine, for which the folding rate constant strongly decreases and eventually saturates at a high concentration (see Figure 4). Of key importance, the corresponding rate constant for TL−TLR *unfolding* also increases substantially with arginine concentration, the synergistic combination of effects resulting in particularly strong destabilization of the folded state by arginine. The simplest interpretation of our data, consistent with the studies of Yarus and co-workers, would be that the guanidine moiety in arginine is responsible for destabilization of the TL−TLR. However, as the pK_a of the guanidine residue in arginine is 12.5 and is therefore fully protonated under neutral pH conditions, it could be that charge alone in the side chain might prove similarly effective at promoting inhibition. Therefore, we have performed similar single-molecule FRET control studies of the TL−TLR construct as a function of lysine (see Figure 4), which has a similarly high side chain p*K*a of 10.5 and thus is also fully protonated. These studies reveal nearly identical levels of amino acid sensitivity on the *folding* process but now with a negligible effect on the *unfolding* kinetics. Hence, it would appear that both charged guanidine and primary amine moieties influence the TL−TLR interaction stability, although more efficiently for arginine.

To test for the possible impact of an uncharged side chain by itself, we further removed the positively charged long-chain residue and probed for the influence of glycine on TL−TLR folding and unfolding rates and stabilities. Surprisingly (see Figure 4c), for complete removal of the positively charged long-chain residue, one still notes a very significant impact of this simplest amino acid at slowing tertiary folding, although requiring a substantially higher concentration (e.g., $1/K_f^{Gly}$ = 250(62) vs $1/K_f^{Arg}$ = 31(11) mM) to achieve a comparable effect. Furthermore, glycine shows essentially no impact on the corresponding unfolding rate constants, quite similar to the effects of lysine (Figure 4b) and yet quite distinctly different from the effects of arginine on single-molecule unfolding events (Figure 4a).

Although each of the three amino acids clearly exerts different fingerprints of influence on the folding/unfolding stability of the TL−TLR tertiary interaction, we offer the following unifying observations: (1) The impact of amino acids on stability for this fundamental RNA tertiary interaction is significant, with up to as much as a three- to fourfold dynamic range in the equilibrium and/or folding/unfolding rate constants. (2) Destabilization of the TL−TLR is evidenced predominantly by a dramatic decrease in the folding rate constants, although with additional, more amino acid specific contributions to acceleration of the unfolding rate processes. (3) The presence of arginine has a particularly strong effect on destabilizing the TL−TLR, in agreement with previous studies on amino acid inhibited self-splicing in the *Tetrahymena* ribozyme.[33,35] (4) By the variety of concentration dependences observed in the four-state kinetic model fits, there would appear to be more than one physical mechanism by which amino acids can destabilize the tertiary interaction.

The unambiguous influence of glycine on the stability of such a tertiary interaction is quite surprising. Indeed, this suggests that destabilization of the TL−TLR is at least not exclusively arising from the charge, pK_a, isolectronic point, or structure of the residue itself but may have additional contributions simply from the α-amine and/or carboxylic acid groups present in all natural amino acids. To explore this further, we have extended these single-molecule FRET studies to two more (non-natural) amino acids, namely, betaine (Bet) and proline (Pro) (Figure 1b). Betaine is quite similar to glycine in structure but with the primary α-amine replaced with a positively charged trimethylamine group. As a function of increasing betaine concentration, modest changes in the folding/unfolding rate constants (17%/25%) and equilibrium constant (40%) are observed (Figure 9),

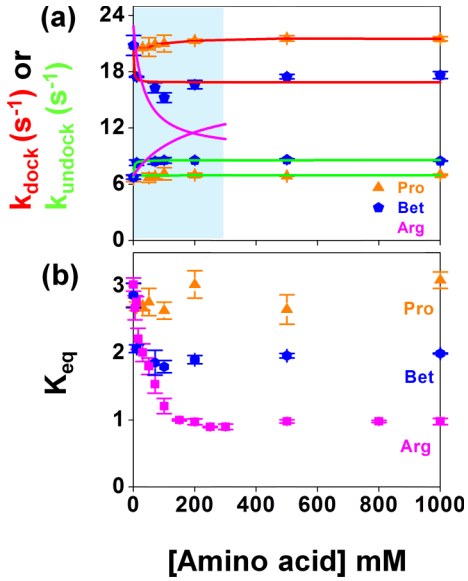

Figure 9. (a) Folding (k_{dock}) and unfolding (k_{undock}) rate constants of TL−TLR RNA plotted as a function of proline (Pro) and betaine (Bet) concentrations, with the previously fitted arginine folding and unfolding rate constants (<300 mM) replotted from Figure 4. Least squares fits (solid lines) are to the four-state kinetic model shown in Figure 5. (b) Folding equilibrium constant (K_{eq}) for TL−TLR RNA plotted as a function of proline and betaine concentrations, with the original arginine-concentration-dependent data replotted for comparison.

that is, less than that observed for glycine or lysine but nearly a factor of twofold less than that with arginine. In conjunction with the effects of lysine on the folding rate constant, this suggest that destabilization of the TL−TLR might occur also as a result of primary amine groups, charged or uncharged, either on the residue or intrinsic to the amino acid itself. The partial loss of activity in betaine might therefore reflect steric effects due to bulky trimethyl substitution of the α-amine, lack of a lone pair, and/or the presence of a unit positive charge. An interesting control test is therefore proline, for which the carboxylic acid group is still present but with the α-amine group

DOI: 10.1021/acs.jpcb.6b05840
J. Phys. Chem. B 2016, 120, 10615−10627

constrained due to incorporation in a five-membered ring. As shown in Figure 9, proline concentration exhibits essentially no impact on the folding/unfolding rate (<5%) and equilibrium constants (<10%), that is, further highlighting the likely additional contribution of even uncharged primary α-amines in destabilizing the TL−TLR tertiary interaction.

IV.B. Enthaplic, Entropic, and Free-Energy Landscapes for TL−TLR Docking. The free-energy landscape for TL−TLR RNA folding with (100 mM) and without amino acids is shown in Figure 10a, where U, TS, and D represent the unfolded, transition, and folded states, respectively. The equilibrium and transition-state free-energy changes are obtained from temperature-dependent studies of the equilibrium constant (Figure 7) and folding rate constant (Figure 8), respectively. As the thermodynamic parameters are sensitive only to differences, for visual simplicity, the zero of energy is arbitrarily referenced to each of the fully unfolded states (U).

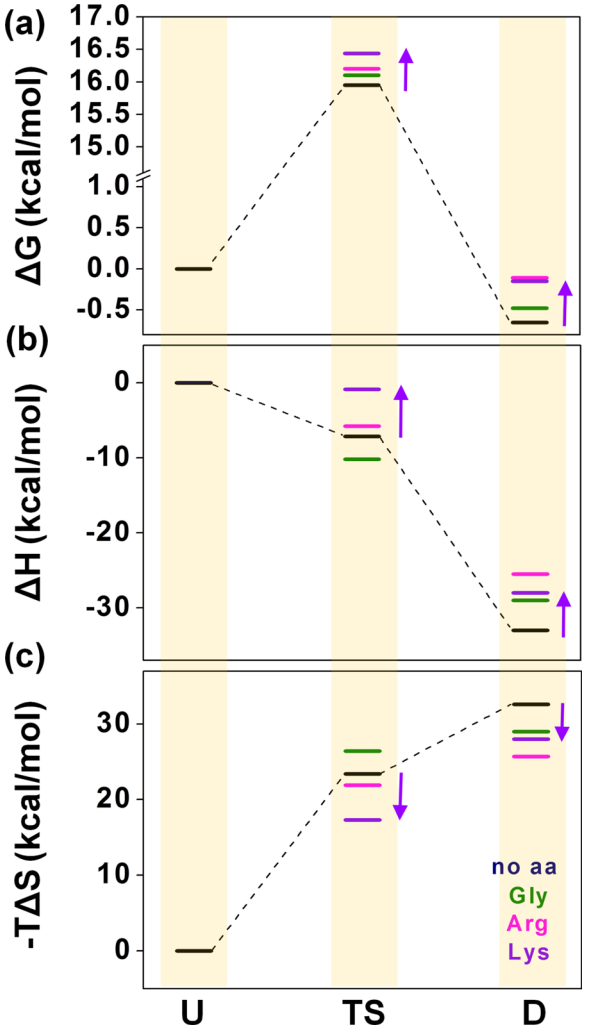

Figure 10. Energy landscape of TL−TLR folding: (a) free energy, (b) enthalpy, and (c) entropy contributions, with (100 mM) and without (0 mM) amino acid. The violet arrow specifically highlights the direction of changes observed for lysine, which is characteristic of a competition between enthalpically destabilizing ($\Delta\Delta H > 0$) and entropically stabilizing ($-T\Delta\Delta S < 0$) effects. The overall destabilization of the transition state and folded conformations by lysine (and arginine) indicates that such effects are dominated by enthalpic contributions.

The overall free-energy change ($\Delta G^\circ = -0.65(3)$ kcal/mol) between the unfolded and folded states of the TL−TLR (in black) is comparable to kT and is also consistent with an approximately equal population in both states. In the presence of Mg^{2+}, many other tertiary interaction motifs, like the P1 helix and P4−P6 domain in the *Tetrahymena* ribozyme and hairpin ribozyme and the 3WJ domain in the Hammerhead ribozyme, are known to show similar changes in the overall free-energy value.[54] In the presence of amino acids, however, the equilibrium constants decrease as the free-energy change systematically shifts upward ($\Delta\Delta G^\circ > 0$) by a modest but clearly. The effect is most pronounced for lysine and arginine ($\Delta\Delta G^\circ = +0.51(4)$ and $+0.54(6)$ kcal/mol) but is also quite appreciable for glycine ($\Delta\Delta G^\circ = +0.20(5)$ kcal/mol), and in all cases, it corresponds to *amino acid induced inhibition* of the TL−TLR equilibrium. In the context of transition state theory, the experimentally observed impact of amino acids on the rate constants can be used to extract the changes in the free-energy barrier to folding and/or unfolding events. In the absence of any amino acid, the free-energy barrier for TL−TLR folding is quite large ($\Delta G^\ddagger = +15.9(6)$ kcal/mol) compared to kT, which results in rate constants on the ms^{-1} to s^{-1} scale. The absolute value of the barrier will scale logarithmically with the assumed attempt frequency ($\nu \approx 10^{13}$ s^{-1}),[67,68] but the observed decrease in rate constant unambiguously indicates an observable increase in the height of this barrier ($\Delta\Delta G_f^\ddagger > 0$) in the presence of arginine ($\Delta\Delta G_f^\ddagger = 0.32(7)$ kcal/mol), lysine ($\Delta\Delta G_f^\ddagger = 0.53(8)$ kcal/mol), and glycine ($\Delta\Delta G_f^\ddagger = 0.20(5)$ kcal/mol). This necessarily implies a systematic amino acid induced slowing of the folding rate process. By way of contrast, free-energy barriers for the unfolding process reveal less sensitivity to amino acid identity. For example, changes in the unfolding barriers are much lower than kT for both lysine ($\Delta\Delta G_u^\ddagger = 0.076(2)$ kcal/mol) and glycine ($\Delta\Delta G_u^\ddagger = -0.068(1)$ kcal/mol) and, although larger, they are still relatively modest for arginine ($\Delta\Delta G_u^\ddagger = -0.445(1)$ kcal/mol). In all cases, the changes in the forward (folding) barrier considerably exceed those in the reverse (unfolding) barrier, which physically means that such amino acid induced inhibition effects are dominated by a decrease in the *folding* rate constants.

For further insight into the amino acid induced destabilization of the TL−TLR tertiary interaction, the free-energy changes have been separated into enthalpic and entropic contributions, as shown in Figure 10b,c, respectively. In the absence of any amino acid, the baseline equilibrium folding of the TL−TLR (shown in black) is quite exothermic ($\Delta H^\circ = -33.1(13)$ kcal/mol) and entropically costly ($\Delta S^\circ = -110.4(44)$ cal/mol K), in agreement with previous studies.[53−55,58,59,64] It also ensures that replacement of the linker by $(PEG)_6$ does not affect the thermodynamic properties of TL−TLR. The exothermicity implies that new hydrogen-bonding and stacking interactions are established in the folded state. Conversely, the high entropic cost suggests that the fully formed TL−TLR tertiary interaction is substantially more compact and ordered than that in the unfolded state. Interestingly, the presence of amino acids systematically causes the folding event to be less exothermic, that is, $\Delta\Delta H^\circ > 0$ (see Figure 10b and Table 2). Specifically, the largest decrease in exothermicity is observed for arginine ($\Delta\Delta H^\circ = 7.6(2)$ kcal/mol), followed by smaller and nearly equivalent values for lysine ($\Delta\Delta H^\circ = 5.2(15)$ kcal/mol) and glycine ($\Delta\Delta H^\circ = 4(2)$ kcal/mol). The source of these amino acid induced shifts in exothermicity would be interesting to explore with molecular

DOI: 10.1021/acs.jpcb.6b05840
J. Phys. Chem. B 2016, 120, 10615−10627

dynamics force fields.[75] However, one simple picture for such a systematic decrease would be interference with hydrogen-bond formation and/or base stacking within the TL−TLR domain, generated by the positively charged guanidine (amine) moiety in the arginine (lysine) side chain ($pK_a \approx 10-12$) interacting with the negatively charged RNA backbone and thereby restricting access to the most favorable loop−loop interaction geometry.

It is important to stress in this regard that glycine does not contain a positively charged residue under buffer conditions, and yet, its presence clearly destabilizes the TL−TLR folded state, specifically by lowering the folding rate constant. Indeed, the structural simplicity of glycine implies that the amine and/or carboxylic acid group by itself must contribute to TL−TLR destabilization. However, there are also clearly important differences between glycine and arginine behaviors, such as (1) a lack of any impact on the unfolding kinetics and (2) a much slower, concentration-dependent approach to saturation in the folding direction. Indeed, the entropic contribution to TL−TLR folding decreases systematically ($-T\Delta\Delta S^\circ < 0$) with the addition of the amino acid series (Figure 10b, Table 2). Amino acid binding close to the GAAA tetraloop or receptor may hinder the loop−loop interaction and alter the compact nature of the folded state. In addition to conformational effects, release of water upon RNA folding and/or amino acid coordination with the RNA is likely to be a non-negligible contribution to the entropy. When two loops of the TL−TLR move closer and/or an amino acid coordinates to a site, it pushes away the surrounding water, which may significantly contribute to the entropy change of the folding/amino acid associated folding. Interestingly, the presence of any of the three amino acids exhibits some efficacy at destabilizing the folded state. One possible inference would be that both a positively charged side chain and free amino acid functional groups (e.g., lysine, glycine) are important in inhibiting the TL−TLR docking interaction, which we can further test more rigorously with non-natural amino group mimetics.

Achieving the TL−TLR folding transition state is a weakly exothermic ($\Delta H^\ddagger < 0$) but entropically a quite costly ($\Delta S^\ddagger \ll 0$) process, with the free-energy barrier dominated by entropic effects. The weakly exothermic nature suggests that contributions to the overall exothermicity (such as hydrogen-bonding and base-stacking interactions) are still largely unformed[69,76] but with a large decrease in the transition-state entropy due to proximal alignment of the receptor and linker (Figure 1a).[61,77,78,74] The presence of both arginine and lysine diminishes the release of heat into the TS (i.e., $\Delta\Delta H^\ddagger > 0$), most prominently for lysine ($\Delta\Delta H^\ddagger = 7.9(1)$ kcal/mol), which could arise from amino acid induced hindering of hydrogen-bond formation and stacking interactions. Such arginine- and lysine-mediated lowering of the heat release would likely be correlated with the formation of a looser transition state, for which one expects, and indeed observes, a corresponding amino acid induced reduction in the entropic barrier ($-T\Delta\Delta S^\ddagger < 0$).

It is worth noting that the effect on TL−TLR enthalpic and entropic changes at the TS differs qualitatively between glycine and lysine or arginine. In the presence of glycine, achieving the TS becomes more rather than less exothermic ($\Delta\Delta H^\ddagger = -3(1)$ kcal/mol), which suggests that glycine helps in hydrogen-bond formation and stabilizes stacking interactions in the TL−TLR domain. On the other hand, glycine lowers the TS entropy ($\Delta\Delta S^\ddagger = -11(5)$ cal/mol K) and thus raises the entropic contribution to the TS barrier. Although opposite in sign, such behavior is entirely consistent with the previous interpretation offered for lysine and arginine, that is, glycine makes the transition state become more strongly hydrogen bonded and thus more entropically constrained. Note that, although small compared to the absolute transition-state barrier heights, the magnitude of these thermodynamic changes is more comparable to the effects due to cation concentrations. However, because of the exponential dependence of the rate constants on such thermodynamic energies, the influences can be rather profound.

Simply summarized, all three amino acids result in destabilization of the TS, but each in different ways. The contributions for glycine are dominated by entropy, whereas the effects are enthalpically dominated for arginine and lysine. Lysine achieves this by slowing only the folding rate, whereas arginine does so by destabilizing the TS from both folding and unfolding directions. Although we have offered a heuristic model for these amino acid contributions based on hydrogen bonding and base stacking in the TL−TLR, detailed molecular dynamics calculations could be invaluable in providing a more molecular-scale picture of these thermodynamic properties, toward which we hope these studies may stimulate additional theoretical activity.

IV.C. Structure−Function Relationship of Amino Acid/RNA Tertiary Interactions. Amino acid induced inhibition of TL−TLR folding is clearly related to amino acid structure. For arginine and lysine, the destabilization of both folded and transition states is dominated by enthalpy change. For glycine, on the other hand, destabilization of the folded state arises enthalpically, with TS shifts dominated by entropy contributions. Positively charged side chain residues, as well as neutral amine functional groups, would appear to play a role in this destabilization. Arginine (Figure 1b) has a large, extended, and positively charged side chain, with a π-electron system and capable of forming strong hydrogen bonds, all properties useful for binding in the TLR nucleotide pocket.

Different amino acid interaction mechanisms for different RNA sequences are common in the literature. In the arginine−aptamer complex,[31] for example, the guanidinium group forms H-bonds with a cage of nucleobases, whereas the α-amine group tends to form a H-bond with the backbone ribose. In the arginine−TAR RNA complex,[32] on the other hand, the guanidinium moiety stacks under the nucleotide and pairs with the G base lying below. Lysine (Figure 1b) exhibits properties similar to those of arginine but contains a cationic primary amine residue. In the SAM 1 riboswitch, the lysine amino group forms a H-bond with the ribose oxygen,[79] whereas the aliphatic side chain binds between two purine bases.[29,30]

Interestingly, glycine has not been tested for impact on the full *Tetrahymena* ribozymal splicing pathway, yet our studies reveal it to be comparably effective to arginine and lysine in the inhibition of TL−TLR folding. The present work clearly provides motivation for such additional studies, with a simple prediction that glycine (and, indeed, possibly other amino acids) might result in reduction of the splicing kinetics. Unlike arginine and lysine, glycine does not contain any aliphatic side chain or cationic residue. The effective destabilization of TL−TLR folding by glycine implies that not only the positively charged residue but also the amino acid functional group has the potential to destabilize TL−TLR folding.

As a final comment, we return to a possible connection between the evolutionary appearance of amino acids and the

DOI: 10.1021/acs.jpcb.6b05840
J. Phys. Chem. B 2016, 120, 10615−10627

influence on RNA tertiary folding and function. Although arginine exhibits the strongest effect on the TL−TLR tertiary interaction, the non-negligible effects on folding due to glycine speak to the role of primary α-amine groups present in all amino acids. Betaine (Bet) (Figure 1b) and proline (Pro) (Figure 1b), which contain different linker and hydrocarbon modifications of the α-amine group, explore this point further. In proline, the five-membered carbon ring turns the α-N into a secondary amine. In betaine, the α-N is converted into a quaternary amine by three methyl groups. In both cases, we observe a strong reduction in the destabilization of TL−TLR folding equilibrium with respect to that in glycine. Indeed, the TL−TLR folding/unfolding rate constants (and therefore K_{eq} as well) appear to be completely insensitive to proline concentration. This observation strongly suggests that free primary α-amines bonded with the chiral carbon center play a crucial role in TL−TLR destabilization, for which one might expect that different enantiomers of amino acid would affect the TL−TLR folding differently. In support of such an enantioselective interaction, Yarus and co-workers have shown that L-arginine inhibits the TL−TLR folding more effectively than D-arginine.[33−35] It would be interesting to explore this further at the single-molecule level, specifically whether such enantioselective effects at the complete ribozyme level would be mirrored in the TL−TLR folding kinetics and thermodynamics.

V. SUMMARY AND CONCLUSIONS

The present work explores the kinetic and thermodynamic origins of amino acid inhibited TL−TLR RNA folding at the single-molecule level. All three amino acids (arginine, lysine, glycine) destabilize the TL−TLR tertiary interaction, as evident from the amino acid induced decrease in the equilibrium constant (K_{eq}) for folding. For all three amino acids, the kinetic origin of this inhibition is due primarily to a decrease in the folding rate constant (k_{dock}) rather than an increase in the unfolding rate constant under elevated amino acid concentration conditions, although the effects on the unfolding rate constants are quite minimal for all but arginine. The dependence of folding rate constants, k_{dock}, *decreases* with increasing amino acid and saturates at a high concentration. The amino acid dependence of both folding and unfolding rate constants can be well fit to a four-state kinetic model, on the basis of (1) rapid equilibrium between the free and amino acid associated TL−TLR species, followed by (2) slower kinetics of TL−TLR folding/unfolding from this equilibrium distribution. On the other hand, k_{undock} shows a modest *increase* only with arginine. The equilibrium constant reveals that the free-energy change for folding shifts to a higher value ($\Delta\Delta G^\circ > 0$) and the transition-state free-energy barrier is raised ($\Delta\Delta G^\ddagger > 0$) with amino acids. Analysis of the free-energy change of the folded state shows that TL−TLR folding is exothermic ($\Delta H^\circ < 0$) and entropically costly ($-T\Delta S^\circ > 0$). In the presence of amino acids, the exothermicity of the folded state decreases ($\Delta\Delta H^\circ > 0$). Moreover, the entropic contribution for the TL−TLR folding also decreases ($-T\Delta\Delta S^\circ < 0$) with amino acids. The loss of exothermicity and lowering of entropic contributions correspond to an amino acid induced destabilization of TL−TLR folding. Moreover, we observe a decrease of exothermicity ($\Delta\Delta H^\ddagger > 0$) and reduction of the entropic barrier ($-T\Delta\Delta S^\ddagger < 0$) in the transition state with arginine and lysine. Although it achieves comparable destabilization effects, the behavior with glycine is exactly the opposite; access to the TL−TLR transition state becomes more exothermic ($\Delta\Delta H^\ddagger < 0$) and raises the entropic barrier ($-T\Delta\Delta S^\ddagger > 0$) with increasing glycine. Comparison of enthalpic and enthalpic contributions implies that changes in the TL−TLR TS are enthalpy-dominated for lysine/arginine and entropy-dominated for glycine. We propose a mechanism whereby binding of the amino acid occupies the space between the tetraloop and receptor, hinders the loop−receptor hydrogen-bond formation, and restricts the proximal alignment of the tetraloop and receptor. This combination of enthalpic and entropic changes results in inhibition of the TL−TLR folding dynamics by each of the amino acids studied.

The inhibition of TL−TLR folding depends on the structure of the amino acids. We have observed that amino acids with positively charged side chains (arginine and lysine), a primary α-amine group (glycine), and a trimethyl-substituted positively charged α-amine group (betaine) destabilize TL−TLR folding. Interestingly the special amino acid (proline) with a ring-trapped α-amino group does not affect the TL−TLR folding. Considering the apparent importance of primary α-amine groups, one might expect different amino acid enantiomers to affect TL−TLR folding differently. In the future, it would be interesting to test for the presence of enantioselective effects on the TL−TLR folding event with different amino acid chiralities.

■ ASSOCIATED CONTENT

Supporting Information

The Supporting Information is available free of charge on the ACS Publications website at DOI: 10.1021/acs.jpcb.6b05840.

Fluorescence intensity trajectories and corresponding E_{FRET} trajectories (PDF)

■ AUTHOR INFORMATION

Corresponding Author

*Email: djn@jila.colorado.edu.

Notes

The authors declare no competing financial interest.

■ ACKNOWLEDGMENTS

Funding for this work was provided by the National Science Foundation (CHE 1266416 and PHY 1125844) and the National Institute for Standards and Technology.

■ REFERENCES

(1) Crick, F. Central Dogma of Molecular Biology. *Nature* **1970**, *227*, 561−563.

(2) Re, A.; Joshi, T.; Kulberkyte, E.; Morris, Q.; Workman, C. T. RNA−Protein Interactions: An Overview. In *RNA Sequence, Structure, and Function: Computational and Bioinformatic Methods*; Gorodkin, J., Ruzzo, L. W., Eds.; Humana Press: Totowa, NJ, 2014; pp 491−521.

(3) Dong, H.; Lei, J.; Ding, L.; Wen, Y.; Ju, H.; Zhang, X. MicroRNA: Function, Detection, and Bioanalysis. *Chem. Rev.* **2013**, *113*, 6207−6233.

(4) Miyoshi, K.; Miyoshi, T.; Hartig, J. V.; Siomi, H.; Siomi, M. C. Molecular Mechanisms That Funnel RNA Precursors into Endogenous Small-Interfering RNA and MicroRNA Biogenesis Pathways in Drosophila. *RNA* **2010**, *16*, 506−515.

(5) Serganov, A.; Nudler, E. A Decade of Riboswitches. *Cell* **2013**, *152*, 17−24.

(6) Henkin, T. M. Riboswitch RNAs: Using RNA to Sense Cellular Metabolism. *Genes Dev.* **2008**, *22*, 3383−3390.

(7) Mandal, M.; Breaker, R. R. Gene Regulation by Riboswitches. *Nat. Rev. Mol. Cell Biol.* **2004**, *5*, 451−463.

DOI: 10.1021/acs.jpcb.6b05840
J. Phys. Chem. B 2016, 120, 10615−10627

(8) Steitz, T. A. A Structural Understanding of the Dynamic Ribosome Machine. *Nat. Rev. Mol. Cell Biol.* **2008**, *9*, 242−253.
(9) Lafontaine, D. L. J.; Tollervey, D. The Function and Synthesis of Ribosomes. *Nat. Rev. Mol. Cell Biol.* **2001**, *2*, 514−520.
(10) Moore, P. B. How Should We Think About the Ribosome? *Annu. Rev. Biophys.* **2012**, *41*, 1−19.
(11) Joyce, G. F. The Antiquity of RNA-Based Evolution. *Nature* **2002**, *418*, 214−221.
(12) Orgel, L. E. Prebiotic Chemistry and the Origin of the RNA World. *Crit. Rev. Biochem. Mol. Biol.* **2004**, *39*, 99−123.
(13) *RNA Worlds: From Life's Origins to Diversity in Gene Regulation*, 1st ed.; Atkins, J. F., Gesteland, R. F, Cech, T. R., Eds.; Cold Spring Harbor Laboratory Press, 2011.
(14) Ricardo, A.; Szostak, J. W. Life on Earth: Fresh Clues Hint at How the First Living Organisms Arose from Inanimate Matter. *Sci. Am.* **2009**, *301*, 54−61.
(15) Morit, A. "The Origin of Life" Talkorigins Archive. 2010; Vol. *2015*. http://www.talkorigins.org/faqs/abioprob/originoflife.html.
(16) Powner, M. W.; Gerland, B.; Sutherland, J. D. Synthesis of Activated Pyrimidine Ribonucleotides in Prebiotically Plausible Conditions. *Nature* **2009**, *459*, 239−242.
(17) Cech, T. R. Self-Splicing of Group I Introns. *Annu. Rev. Biochem.* **1990**, *59*, 543−568.
(18) Huang, W.; Ferris, J. P. One-Step, Regioselective Synthesis of up to 50-Mers of RNA Oligomers by Montmorillonite Catalysis. *J. Am. Chem. Soc.* **2006**, *128*, 8914−8919.
(19) Rajamani, S.; Vlassov, A.; Benner, S.; Coombs, A.; Olasagasti, F.; Deamer, D. Lipid-Assisted Synthesis of RNA-Like Polymers from Mononucleotides. *Origins Life Evol. Biospheres* **2008**, *38*, 57−74.
(20) Szostak, J. W.; Bartel, D. P.; Luisi, P. L. Synthesizing Life. *Nature* **2001**, *409*, 387−390.
(21) Lincoln, T. A.; Joyce, G. F. Self-Sustained Replication of an RNA Enzyme. *Science* **2009**, *323*, 1229−1232.
(22) Miller, S. L. A Production of Amino Acids under Possible Primitive Earth Conditions. *Science* **1953**, *117*, 528−529.
(23) Woese, C. R.; Dugre, D. H.; Saxinger, W. C.; Dugre, S. A. The Molecular Basis for the Genetic Code. *Proc. Natl. Acad. Sci. U.S.A.* **1966**, *55*, 966−974.
(24) Orgel, L. E. Evolution of the Genetic Apparatus. *J. Mol. Biol.* **1968**, *38*, 381−393.
(25) Lodish, H.; Berk, A.; Zipursky, S. L.; et al. *The Three Roles of RNA in Protein Synthesis*, 4th ed.; W. H. Freeman: New York, 2000.
(26) Gilbert, S. D.; Rambo, R. P.; Van Tyne, D.; Batey, R. T. Structure of the Sam-Ii Riboswitch Bound to S-Adenosylmethionine. *Nat. Struct. Mol. Biol.* **2008**, *15*, 177−182.
(27) Lu, C.; Smith, A. M.; Fuchs, R. T.; Ding, F.; Rajashankar, K.; Henkin, T. M.; Ke, A. Crystal Structures of the Sam-Iii/Smk Riboswitch Reveal the Sam-Dependent Translation Inhibition Mechanism. *Nat. Struct. Mol. Biol.* **2008**, *15*, 1076−1083.
(28) Montange, R. K.; Batey, R. T. Structure of the S-Adenosylmethionine Riboswitch Regulatory mRNA Element. *Nature* **2006**, *441*, 1172−1175.
(29) Serganov, A.; Huang, L.; Patel, D. J. Structural Insights into Amino Acid Binding and Gene Control by a Lysine Riboswitch. *Nature* **2008**, *455*, 1263−1267.
(30) Garst, A. D.; Héroux, A.; Rambo, R. P.; Batey, R. T. Crystal Structure of the Lysine Riboswitch Regulatory mRNA Element. *J. Biol. Chem.* **2008**, *283*, 22347−22351.
(31) Yang, Y.; Kochoyan, M.; Burgstaller, P.; Westhof, E.; Famulok, M. Structural Basis of Ligand Discrimination by Two Related RNA Aptamers Resolved by NMR Spectroscopy. *Science* **1996**, *272*, 1343−1347.
(32) Puglisi, J. D.; Chen, L.; Frankel, A. D.; Williamson, J. R. Role of RNA Structure in Arginine Recognition of Tar RNA. *Proc. Natl. Acad. Sci. U.S.A.* **1993**, *90*, 3680−3684.
(33) Yarus, M. A Specific Amino Acid Binding Site Composed of RNA. *Science* **1988**, *240*, 1751−1758.
(34) Yarus, M.; Christian, E. L. Genetic Code Origins. *Nature* **1989**, *342*, 349−350.
(35) Yarus, M.; Majerfeld, I. Co-Optimization of Ribozyme Substrate Stacking and L-Arginine Binding. *J. Mol. Biol.* **1992**, *225*, 945−949.
(36) Allers, J.; Shamoo, Y. Structure-Based Analysis of Protein-RNA Interactions Using the Program Entangle1. *J. Mol. Biol.* **2001**, *311*, 75−86.
(37) Hoffman, M. M.; Khrapov, M. A.; Cox, J. C.; Yao, J.; Tong, L.; Ellington, A. D. AANT: The Amino Acid−Nucleotide Interaction Database. *Nucleic Acids Res.* **2004**, *32*, D174−D181.
(38) Kondo, J.; Westhof, E. Classification of Pseudo Pairs between Nucleotide Bases and Amino Acids by Analysis of Nucleotide−Protein Complexes. *Nucleic Acids Res.* **2011**, *39*, 8628−8637.
(39) Morozova, N.; Allers, J.; Myers, J.; Shamoo, Y. Protein−RNA Interactions: Exploring Binding Patterns with a Three-Dimensional Superposition Analysis of High Resolution Structures. *Bioinformatics* **2006**, *22*, 2746−2752.
(40) Rutledge, L. R.; Campbell-Verduyn, L. S.; Hunter, K. C.; Wetmore, S. D. Characterization of Nucleobase−Amino Acid Stacking Interactions Utilized by a DNA Repair Enzyme. *J. Phys. Chem. B* **2006**, *110*, 19652−19663.
(41) Rutledge, L. R.; Campbell-Verduyn, L. S.; Wetmore, S. D. Characterization of the Stacking Interactions between DNA or RNA Nucleobases and the Aromatic Amino Acids. *Chem. Phys. Lett.* **2007**, *444*, 167−175.
(42) Rutledge, L. R.; Durst, H. F.; Wetmore, S. D. Computational Comparison of the Stacking Interactions between the Aromatic Amino Acids and the Natural or (Cationic) Methylated Nucleobases. *Phys. Chem. Chem. Phys.* **2008**, *10*, 2801−2812.
(43) Serganov, A.; Patel, D. J. Ribozymes, Riboswitches and Beyond: Regulation of Gene Expression without Proteins. *Nat. Rev. Genet.* **2007**, *8*, 776−790.
(44) Zhuang, X.; Kim, H.; Pereira, M. J. B.; Babcock, H. P.; Walter, N. G.; Chu, S. Correlating Structural Dynamics and Function in Single Ribozyme Molecules. *Science* **2002**, *296*, 1473−1476.
(45) Tinoco, I., Jr.; Bustamante, C. How RNA Folds. *J. Mol. Biol.* **1999**, *293*, 271−281.
(46) Brion, P.; Westhof, E. Hierarchy and Dynamics of RNA Folding. *Annu. Rev. Biophys. Biomol. Struct.* **1997**, *26*, 113−137.
(47) Das, R.; Kwok, L. W.; Millett, I. S.; Bai, Y.; Mills, T. T.; Jacob, J.; Maskel, G. S.; Seifert, S.; Mochrie, S. G. J.; Thiyagarajan, P.; et al. The Fastest Global Events in RNA Folding: Electrostatic Relaxation and Tertiary Collapse of the Tetrahymena Ribozyme. *J. Mol. Biol.* **2003**, *332*, 311−319.
(48) Russell, R.; Millett, I. S.; Tate, M. W.; Kwok, L. W.; Nakatani, B.; Gruner, S. M.; Mochrie, S. G. J.; Pande, V.; Doniach, S.; Herschlag, D.; et al. Rapid Compaction During RNA Folding. *Proc. Natl. Acad. Sci. U.S.A.* **2002**, *99*, 4266−4271.
(49) O'Connor, D. V.; Phillips, D. *Time-Correlated Single Photon Counting*; Academic Press, 2012.
(50) Batey, R. T.; Rambo, R. P.; Doudna, J. A. Tertiary Motifs in RNA Structure and Folding. *Angew. Chem., Int. Ed.* **1999**, *38*, 2326−2343.
(51) Vander Meulen, K. A.; Davis, J. H.; Foster, T. R.; Record, M. T., Jr.; Butcher, S. E. Thermodynamics and Folding Pathway of Tetraloop Receptor-Mediated RNA Helical Packing. *J. Mol. Biol.* **2008**, *384*, 702−717.
(52) Sattin, B. D.; Zhao, W.; Travers, K.; Chu, S.; Herschlag, D. Direct Measurement of Tertiary Contact Cooperativity in RNA Folding. *J. Am. Chem. Soc.* **2008**, *130*, 6085−6087.
(53) Hodak, J. H.; Fiore, J. L.; Nesbitt, D. J.; Downey, C. D.; Pardi, A. Docking Kinetics and Equilibrium of a GAAA Tetraloop-Receptor Motif Probed by Single-Molecule FRET. *Proc. Natl. Acad. Sci. U.S.A.* **2005**, *102*, 10505−10510.
(54) Fiore, J. L.; Kraemer, B.; Koberling, F.; Edmann, R.; Nesbitt, D. J. Enthalpy-Driven RNA Folding: Single-Molecule Thermodynamics of Tetraloop−Receptor Tertiary Interaction. *Biochemistry* **2009**, *48*, 2550−2558.
(55) Downey, C. D.; Fiore, J. L.; Stoddard, C. D.; Hodak, J. H.; Nesbitt, D. J.; Pardi, A. Metal Ion Dependence, Thermodynamics, and Kinetics for Intramolecular Docking of a GAAA Tetraloop and

DOI: 10.1021/acs.jpcb.6b05840
J. Phys. Chem. B 2016, 120, 10615−10627

Receptor Connected by a Flexible Linker. *Biochemistry* **2006**, *45*, 3664−3673.
(56) Aitken, C. E.; Marshall, R. A.; Puglisi, J. D. An Oxygen Scavenging System for Improvement of Dye Stability in Single-Molecule Fluorescence Experiments. *Biophys. J.* **2008**, *94*, 1826−1835.
(57) Holmstrom, E. D.; Nesbitt, D. J. Real-Time Infrared Overtone Laser Control of Temperature in Picoliter H_2O Samples: "Nano-bathtubs" for Single Molecule Microscopy. *J. Phys. Chem. Lett.* **2010**, *1*, 2264−2268.
(58) Fiore, J. L.; Holmstrom, E. D.; Nesbitt, D. J. Entropic Origin of Mg^{2+}-Facilitated RNA Folding. *Proc. Natl. Acad. Sci. U.S.A.* **2012**, *109*, 2902−2907.
(59) Holmstrom, E. D.; Fiore, J. L.; Nesbitt, D. J. Thermodynamic Origins of Monovalent Facilitated RNA Folding. *Biochemistry* **2012**, *51*, 3732−3743.
(60) Blanco, M.; Walter, N. G. Analysis of Complex Single-Molecule Fret Time Trajectories. In *Methods in Enzymology*; Nils, G. W., Ed.; Academic Press, 2010; Vol. *472*; pp 153−178.
(61) Bartley, L. E.; Zhuang, X.; Das, R.; Chu, S.; Herschlag, D. Exploration of the Transition State for Tertiary Structure Formation between an RNA Helix and a Large Structured RNA. *J. Mol. Biol.* **2003**, *328*, 1011−1026.
(62) Zhou, Y.; Zhuang, X. Robust Reconstruction of the Rate Constant Distribution Using the Phase Function Method. *Biophys. J.* **2006**, *91*, 4045−4053.
(63) Kim, H. D.; Nienhaus, G. U.; Ha, T.; Orr, J. W.; Williamson, J. R.; Chu, S. Mg^{2+}-Dependent Conformational Change of RNA Studied by Fluorescence Correlation and Fret on Immobilized Single Molecules. *Proc. Natl. Acad. Sci. U.S.A.* **2002**, *99*, 4284−4289.
(64) Fiore, J. L.; Hodak, J. H.; Piestert, O.; Downey, C. D.; Nesbitt, D. J. Monovalent and Divalent Promoted GAAA Tetraloop-Receptor Tertiary Interactions from Freely Diffusing Single-Molecule Studies. *Biophys. J.* **2008**, *95*, 3892−3905.
(65) Grote, R. F.; Hynes, J. T. The Stable States Picture of Chemical Reactions. Ii. Rate Constants for Condensed and Gas Phase Reaction Models. *J. Chem. Phys.* **1980**, *73*, 2715−2732.
(66) Kramers, H. A. Brownian Motion in a Field of Force and the Diffusion Model of Chemical Reactions. *Physica* **1940**, *7*, 284−304.
(67) Zwanzig, R.; Szabo, A.; Bagchi, B. Levinthal's Paradox. *Proc. Natl. Acad. Sci. U.S.A.* **1992**, *89*, 20−22.
(68) Szabo, A.; Schulten, K.; Schulten, Z. First Passage Time Approach to Diffusion Controlled Reactions. *J. Chem. Phys.* **1980**, *72*, 4350−4357.
(69) Cate, J. H.; Gooding, A. R.; Podell, E.; Zhou, K.; Golden, B. L.; Kundrot, C. E.; Cech, T. R.; Doudna, J. A. Crystal Structure of a Group I Ribozyme Domain: Principles of RNA Packing. *Science* **1996**, *273*, 1678−1685.
(70) Zarrinkar, P. P.; Williamson, J. R. The Kinetic Folding Pathway of the Tetrahymena Ribozyme Reveals Possible Similarities between RNA and Protein Folding. *Nat. Struct. Mol. Biol.* **1996**, *3*, 432−438.
(71) Lafontaine, D. A.; Norman, D. G.; Lilley, D. M. Structure, Folding and Activity of the vs Ribozyme: Importance of the 2-3-6 Helical Junction. *EMBO J.* **2001**, *20*, 1415−1424.
(72) Golden, B. L.; Hammes-Schiffer, S.; Carey, P. R.; Bevilacqua, P. C. An Integrated Picture of HDV Ribozyme Catalysis. In *Biophysics of RNA Folding*; Russell, R., Ed.; Springer: New York, NY, 2013; pp 135−167.
(73) Zhang, S.; Ganguly, A.; Goyal, P.; Bingaman, J. L.; Bevilacqua, P. C.; Hammes-Schiffer, S. Role of the Active Site Guanine in the glms Ribozyme Self-Cleavage Mechanism: Quantum Mechanical/Molecular Mechanical Free Energy Simulations. *J. Am. Chem. Soc.* **2015**, *137*, 784−798.
(74) Young, B. T.; Silverman, S. K. The GAAA Tetraloop−Receptor Interaction Contributes Differentially to Folding Thermodynamics and Kinetics for the P4−P6 RNA Domain. *Biochemistry* **2002**, *41*, 12271−12276.
(75) Banáš, P.; Hollas, D.; Zgarbová, M.; Jurečka, P.; Orozco, M.; Cheatham, T. E.; Šponer, J.; Otyepka, M. Performance of Molecular Mechanics Force Fields for RNA Simulations: Stability of UUCG and GNRA Hairpins. *J. Chem. Theory Comput.* **2010**, *6*, 3836−3849.
(76) Butcher, S. E.; Dieckmann, T.; Feigon, J. Solution Structure of a GAAA Tetraloop Receptor RNA. *EMBO J.* **1997**, *16*, 7490−7499.
(77) Bokinsky, G.; Rueda, D.; Misra, V. K.; Rhodes, M. M.; Gordus, A.; Babcock, H. P.; Walter, N. G.; Zhuang, X. Single-Molecule Transition-State Analysis of RNA Folding. *Proc. Natl. Acad. Sci. U.S.A.* **2003**, *100*, 9302−9307.
(78) Maglott, E. J.; Goodwin, J. T.; Glick, G. D. Probing the Structure of an RNA Tertiary Unfolding Transition State. *J. Am. Chem. Soc.* **1999**, *121*, 7461−7462.
(79) Sudarsan, N.; Wickiser, J. K.; Nakamura, S.; Ebert, M. S.; Breaker, R. R. An mRNA Structure in Bacteria That Controls Gene Expression by Binding Lysine. *Genes Dev.* **2003**, *17*, 2688−2697.

DOI: 10.1021/acs.jpcb.6b05840
J. Phys. Chem. B 2016, 120, 10615−10627